Effect of Shape Memory Alloy on Seismic Performance and Residual Drift Reduction in Steel Frames Equipped with Mega-Braces

M. Shahrjerdi *, Mir Hamid Hoseini , Armin Azimi Nejhad , Alireza Anisi

Posted Date: 16 April 2026

doi: 10.20944/preprints202604.1181.v1

Keywords: shape memory alloy (SMA); mega-brace; residual drift; seismic performance; nonlinear dynamic analysis; ABAQUS; steel structures

 doi:10.20944/preprints202604.1181.v1

Article

Effect of Shape Memory Alloy on Seismic Performance and Residual Drift Reduction in Steel Frames Equipped with Mega-Braces

M. Shahrjerdi [1], Mir Hamid Hoseini [2], Armin Azimi Nejhad [2] and Alireza Anisi [3,*]

[1] AMIMechE, Brighton, UK

[2] Faculty of Civil Engineering, Architecture and Art, Science and Research Branch, Islamic Azad University (IAU), Tehran, Iran

[3] Faculty of Architecture and Art, Science and Research Branch, Islamic Azad University (IAU), Tehran, Iran

* Correspondence: m.shahrjerdi@outlook.com

Abstract

Reducing residual drifts and maintaining post–earthquake functionality have become key requirements in performance-based seismic design. In this study, the seismic behavior of three steel frame models 2, 3, and 6-story configurations equipped with eight-shaped mega-braces with and without Shape Memory Alloy (SMA) components was evaluated using nonlinear explicit dynamic analysis in ABAQUS. The main innovation of this research lies in the simultaneous integration of SMA elements into the mega-brace system and in analyzing their effects on residual drift, plastic strain, and response modification factor (R) through detailed three-dimensional numerical modeling. Results show that the use of SMA reduces peak von Mises stress by 2–3% and decreases plastic strain by 7% in the 2-story model, 50% in the 3-story model, and 55% in the 6-story model. The most significant finding is the 99.99% reduction in residual drift across all models, demonstrating highly effective self-centering behavior. The evaluation of the response modification factor revealed that SMA increases R by 42% in the 2-story model, decreases it by 23% in the 3-story model, and in the 6-story frame results in a 5% increase for the two-story bracing configuration and a 34% decrease for the three-story bracing configuration. These results indicate that although SMA reduces hysteretic energy dissipation in some cases, it significantly enhances the seismic performance of the mega-brace system by virtually eliminating permanent deformation, reducing stress concentration, improving cyclic stability, and effectively controlling inelastic displacements. Therefore, incorporating SMA into mega-brace systems can serve as an efficient approach for structures where maintaining functionality and usability after an earthquake is a critical priority.

Keywords: shape memory alloy (SMA); mega-brace; residual drift; seismic performance; nonlinear dynamic analysis; ABAQUS; steel structures

1. Introduction

Performance-based seismic design has recently placed particular emphasis on reducing residual displacements and preserving the post-earthquake serviceability of structures. Within this framework, structural response beyond peak loading including unloading behavior and self-centering capacity is considered a key performance indicator, in addition to the control of forces and maximum deformations. Mega-bracing systems have attracted considerable attention in recent years owing to their adequate lateral stiffness, efficient force distribution along the height, and ability to establish stable load paths. However, their nonlinear behavior is typically associated with the development of plastic strains and permanent deformations. In contrast, shape memory alloys (SMAs) present a promising solution for mitigating cumulative damage and enhancing structural self-centering capability during seismic events, thanks to their superelastic behavior, stable hysteretic

 doi:10.20944/preprints202604.1181.v1

loops, and ability to recover their original shape upon unloading. Previous studies have predominantly focused on the application of SMAs in conventional bracing systems or localized connections, while limited research has investigated the integration of SMAs with mega-bracing configurations and their influence on critical performance indices such as residual drift, plastic strain demand, and behavior factor. Moreover, much of the existing work has relied on limited experimental investigations or has not examined system behavior at the full structural scale within detailed three-dimensional numerical models.

The integration of SMA elements with bracing systems is implemented by connecting vertical SMA members to the primary braces in a manner that exploits the superelasticity and shape recovery characteristics of SMAs to enhance seismic performance. In this configuration, SMA bars are installed vertically alongside the main braces such that they undergo axial tension or compression under lateral seismic loads. Their ends are anchored to bracing connection nodes—such as gusset plates at beam interfaces via high-strength end plates. During seismic excitation, the SMA elements elongate and, owing to their superelastic response, recover their deformation upon load reduction, thereby returning the structure toward its initial position. To prevent lateral buckling and corrosion, SMA bars are typically housed within protective tubes. Furthermore, connections must be designed with capacities exceeding the tensile strength of the SMA material to ensure that failure occurs within the SMA element itself rather than at the connection. This system significantly improves structural ductility and self-centering capability while maintaining adequate strength [2].

Designing structures to remain fully elastic under severe earthquakes is economically impractical; consequently, passive structural control strategies have been widely adopted. These approaches intentionally allow certain structural components to sustain damage during strong ground motions in order to reduce demands on primary load-bearing elements such as columns. Nevertheless, all currently employed energy-dissipating systems present drawbacks—not only in terms of cost, but also regarding limited service life, fatigue susceptibility, installation complexity, the need for post-earthquake replacement, and alterations to the original structural geometry [3]. Mega-bracing systems represent an advanced configuration that integrates conventional bracing elements such that the structure behaves as a single, unified bracing unit akin to a "mega" diagonal spanning multiple stories. Conventional bracing systems employed in steel structures today are typically confined to a single story and a single bay. In contrast, mega-bracing significantly expands the scale of bracing action, enabling a single brace to extend vertically across multiple stories within one bay or horizontally across multiple bays within a single story. The fundamental function of these systems, similar to other bracing types, is to provide the necessary lateral stiffness to the structural system. Mega-bracing systems are particularly justified in high-rise buildings; however, they are generally not economically viable for low- to mid-rise structures where conventional concentric or eccentric bracing systems suffice. These configurations, commonly referred to as "super-braces" or "mega-braces," have been implemented in various landmark structures [4].

In light of the above, the present study investigates the influence of shape memory alloy (SMA) elements on seismic response parameters in three-dimensional steel structures equipped with chevron-type mega-braces. The models feature a 5-meter bay width with mega-bracing repetitions spanning either two or three stories within a single bay. To address existing research gaps, the seismic behavior of three steel building models 2, 3, and 6-story frames with chevron mega-braces, both with and without SMA elements is evaluated through explicit dynamic analysis in ABAQUS. The primary focus lies on elucidating the mechanism by which SMA elements contribute to: (i) control of residual displacements, (ii) reduction of plastic strain demands, (iii) enhancement of hysteretic stability, and (iv) modification of the behavior factor.

For the first time, this research simulates 2, 3, and 6-story steel structures incorporating chevron mega-braces integrated with SMA elements under explicit dynamic analysis in ABAQUS, comprehensively assessing their seismic performance, plastic strain distribution, stress patterns, and self-centering capability. The principal innovation of this work resides in this novel SMA–mega-brace hybridization implemented within a realistic three-dimensional modeling framework. The findings

 doi:10.20944/preprints202604.1181.v1

establish a foundation for designing highly reliable self-centering structures where post-earthquake functionality is of critical importance, thereby advancing performance-based seismic design toward more resilient and serviceable structural systems.

2. Literature Review

Khodabandehloo (2024) proposed four steel concentrically braced frame models incorporating curvilinear braces arranged in distinct geometric patterns and evaluated their seismic behavior in a two-story structure. The designed models were subjected to lateral and cyclic loading via finite element analysis, and their load-carrying capacity, seismic response, ductility, seismic energy dissipation, behavior factor, stiffness degradation, failure mode, and economic index were comparatively assessed [4].

Ghasemieh and Mardi (2023) compared the seismic performance of structures equipped with buckling-restrained braces (BRBs) against those braced with iron-based and nickel-based shape memory alloy (SMA) elements. The systems were modeled in SeismoStruct, and incremental dynamic analysis was performed on a seven-story structure with chevron bracing. Results indicated that structures braced with iron-based SMAs exhibited lower peak and residual displacements and superior overall performance compared to those braced with Nitinol. However, iron-based SMA-braced frames experienced larger peak displacements than BRB-braced frames, while leaving virtually no residual displacement [5]. Bagheri et al. (2020) evaluated the seismic performance of dual steel moment-resisting frames with eccentric braces incorporating SMA rods at the ends of bracing members. A five-story steel dual system was modeled and subjected to nonlinear time-history dynamic analysis. Structural responses including maximum absolute roof displacement, interstory drifts, residual roof displacement, base shear, and peak roof acceleration were systematically assessed [6]. Danesh and Jafari (2020) investigated the effect of SMA-equipped connections on superelastic vibration control. The behavior of an eight-bolt rigid connection fitted with superelastic Nitinol bolts was examined via finite element analysis and compared with an identical connection using conventional high-strength bolts. Both connection types were analyzed under various earthquake records, and structural response curves—including displacement, residual displacement, and base shear—were extracted. Results demonstrated that while the high-strength bolted connection exhibited high ductility and good energy dissipation, it suffered significant residual deformations, rendering it essentially non-repairable after seismic events. In contrast, the Nitinol-bolted connection, while maintaining good damping and ductility, displayed excellent recentering capability, thereby reducing structural damage [7]. Zhu et al. (2021) examined buckling-restrained mega-braces in which the BRB serves as a high-performance seismic-resistant element that not only enhances strength and stiffness but also provides excellent energy absorption capacity. Since its emergence in the late 1980s, the BRB has been the subject of extensive research. Various BRB configurations have been proposed by researchers and practitioners—primarily in Japan, the United States, and China—to address diverse structural requirements. Ongoing research continues to focus on developing BRBs that are more efficient, compact, lightweight, cost-effective, and easier to install. This study summarizes BRB development over recent decades, including historical evolution, classification, applications, and scientific advancements, while discussing the advantages of different BRB types and offering insights into future prospects [8]. Jia et al. (2022) introduced a novel self-centering SMA-based brace that simultaneously enhances energy dissipation capacity and reduces residual deformation in civil structures by integrating SMA superelasticity with low-friction sliding mechanisms. Seven self-centering SMA brace specimens were tested under cyclic loading, and their performance characteristics—including hysteretic loops, force–displacement curves, secant stiffness, equivalent damping ratio, energy consumption coefficient, and self-centering ratio—were evaluated. Experimental findings revealed that these braces exhibited high energy dissipation capacity, adequate strength, and remarkable self-centering ability: steel plates remained elastic throughout testing, and SMA elements subjected solely to tension fully recovered their original configuration. All specimens displayed flag-shaped hysteretic loops with minimal residual drift, achieving a self-

 doi:10.20944/preprints202604.1181.v1

centering ratio as high as 89.38%. Loading rate and initial strain were also found to significantly influence seismic performance. To simulate the brace's seismic behavior, an enhanced numerical model was developed in MATLAB by combining the Graesser and Buc–Wen models. Numerical results showed good agreement with experimental data under identical conditions, confirming the model's accuracy in predicting the seismic response of the proposed self-centering SMA brace [9]. Jena et al. (2025) investigated the seismic performance of iron-based SMA (Fe-SMA) buckling-restrained braces as a novel alternative to conventional steel braces. Since conventional steel braces, owing to their low post-yield stiffness, often induce significant residual drifts after seismic events, Fe-SMA—with its higher post-yield stiffness—presents a promising solution. In this numerical study, a hybrid BRB core composed of Fe-SMA was arranged in series with an elastic segment to enhance the system's overall post-yield stiffness. The seismic performance of 3-, 9-, and 20-story frames equipped with these braces—under both rigid and pinned beam–column connections—was analyzed in OpenSees using 20 pairs of near-fault and far-fault earthquake records. Results demonstrated that Fe-SMA-braced frames significantly reduced residual drifts compared to both conventional steel and hybrid steel braces, particularly under near-fault ground motions where residual drifts are typically exacerbated. Frames with rigid connections exhibited the lowest residual and peak interstory drift demands. Although hybrid braces experienced higher ductility demands, the superior fatigue life of Fe-SMA establishes it as a suitable material for BRB core applications [10].

3. Model Description

The steel material properties adopted in this study are presented in Table 1.

Table 1. Mechanical properties of structural steel (St37) [11].

Material	Yield Stress (kg/cm²)	Ultimate Stress (kg/cm²)	Poisson's Ratio
Steel (St37)	2400	3700	0.3

The data in Table 1 characterizes material behavior within the elastic deformation range. However, upon reaching the yield point, the material response becomes nonlinear, necessitating additional constitutive parameters to accurately model post-yield behavior. As noted earlier, post-yield material characteristics are typically derived from tensile coupon tests. Table 2 presents the plasticity parameters for St37 steel employed in the numerical simulations.

Table 2. Plasticity parameters for St37 steel [11].

Plastic Strain	Yield Stress (MPa)
0.00	235
0.28	363

Note: Values converted from original units (2400 kg/cm² ≈ 235 MPa; 3700 kg/cm² ≈ 363 MPa) for consistency with international standards.

Figure 3 illustrates the superelastic behavior of shape memory alloys based on cyclic force–displacement response. The left diagram (Figure 3a) presents experimental force–displacement data obtained from tensile tests on NiTi wires conducted at the University of Basilicata. The right diagram (Figure 3b) schematically depicts the idealized force–displacement relationship implemented in the numerical analyses, derived from the aforementioned experimental results [12]. This constitutive representation captures the characteristic flag-shaped hysteresis loop, negligible residual deformation, and self-recovery capability inherent to superelastic SMAs under cyclic loading.

 doi:10.20944/preprints202604.1181.v1

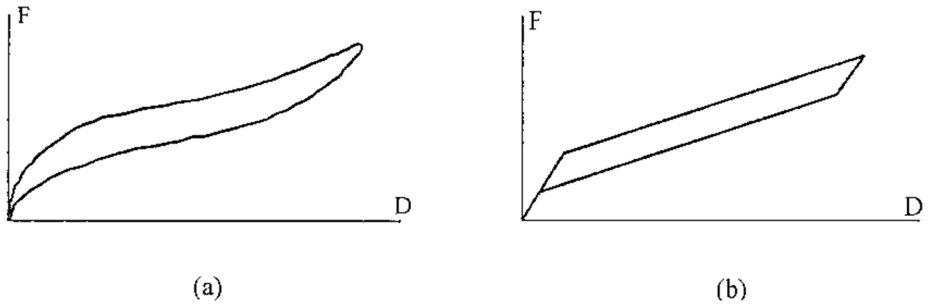

Figure 1. Force–displacement relationship for SMAs based on experimental results (a) and corresponding numerical model (b) [12].

As evident from the figure, the mechanical response of these materials is governed by internal phase transformations. Both the forward phase transformation (austenite to martensite) and the reverse transformation (martensite to austenite) occur during cyclic loading and unloading. These reversible solid-state phase transitions constitute the fundamental mechanism underlying the superelastic behavior of shape memory alloys [13].

NiTi (Nickel–Titanium) wires were adopted as SMA elements in this study, with the following mechanical properties considered in the numerical modeling (Figure 2):

- Material composition: Near-equiatomic NiTi (50.8 at.% Ni)
- Transformation temperatures: Austenite finish temperature (*Af*) ≈ 35 °C; Martensite start temperature (*Ms*) ≈ 15 °C
- Superelastic plateau stress: 450–550 MPa (loading); 250–350 MPa (unloading)
- Recoverable strain: Up to 8%
- Elastic modulus: ~70 GPa (austenitic phase); ~28 GPa (martensitic phase)
- Poisson's ratio: 0.33
- Density: 6450 kg/m³

These parameters were implemented in the ABAQUS user material subroutine (UMAT) to capture the characteristic flag-shaped hysteresis, stress plateaus associated with phase transformations, and near-complete strain recovery upon unloading.

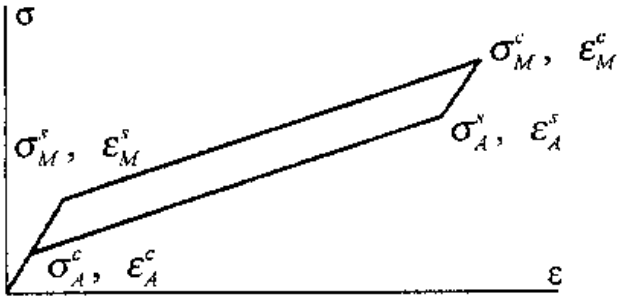

Figure 2. Mechanical properties of NiTi wires [13].

The mechanical behavior of shape memory alloys is governed by reversible solid-state phase transformations. During cyclic loading, the forward transformation (austenite → martensite) and reverse transformation (martensite → austenite) occur sequentially, forming the physical basis of superelasticity in SMAs [13].

NiTi wires were selected as SMA elements with mechanical characteristics defined according to experimental data from the University of Basilicata (Table 3).

 doi:10.20944/preprints202604.1181.v1

Table 3. Stress–strain characteristics of SMA material from tensile tests at the University of Basilicata [14].

Diagram point	Description	Stress (MPa)	Strain
Point As	Start of austenite → martensite transformation	165	0.0045
Point Af	Finish of austenite → martensite transformation	280	0.0070
Point Ms	Start of martensite → austenite transformation	390	0.0595
Point Mf	Finish of martensite → austenite transformation	525	0.0660

Note: Symbols As, Af, Ms, and Mf denote the stress and strain values corresponding to the start and finish of forward (austenite→martensite) and reverse (martensite→austenite) phase transformations, respectively, as obtained from experimental investigations at the University of Basilicata [14].

Material properties for the SMA alloy were implemented in ABAQUS through a user-defined material subroutine (UMAT). The subroutine was coded in Fortran and linked to the analysis via the *Job* module using the *Write Input* option to generate a text-based input file incorporating the UMAT definition [18]. ABAQUS/Explicit version 2017 was employed to facilitate subroutine-based modeling of SMA constitutive behavior [15]. Steel material properties were also defined within the UMAT framework using Python scripting libraries accessible through the *Job* module to ensure consistent nonlinear material representation [16].

In the SMA–mega-brace hybrid systems investigated herein, connections were modeled as either pinned or semi-rigid joints, depending on the intended structural response and the axial-dominated behavior of SMA elements. This modeling approach accurately captures the force transfer mechanism while allowing controlled rotational freedom at brace–beam–column intersections.

Three-dimensional finite element models were developed with uniform story height of 3.0 m and a single bay width of 5.0 m. Three building configurations were analyzed: 2-, 3-, and 6-story steel frames. Within each configuration, mega-bracing systems spanned either two or three consecutive stories within the single bay, forming chevron-type mega-brace arrangements. Figures 3–6 illustrate the 3D structural models, where chevron braces are represented by truss elements and vertical SMA elements are positioned centrally alongside the bracing system.

As depicted in Figure 3 (left), the SMA elements were implemented as two vertical tension-only members installed parallel to the chevron braces. Under lateral seismic loading, one diagonal brace experiences tension while the other undergoes compression; simultaneously, the vertical SMA elements are elongated in tension. Upon load removal, the superelastic recovery of the SMA elements releases the stored tensile strain and actively re-centers the structure toward its original position. This mechanism effectively mitigates residual interstory drifts while maintaining the energy dissipation capacity of the conventional bracing system.

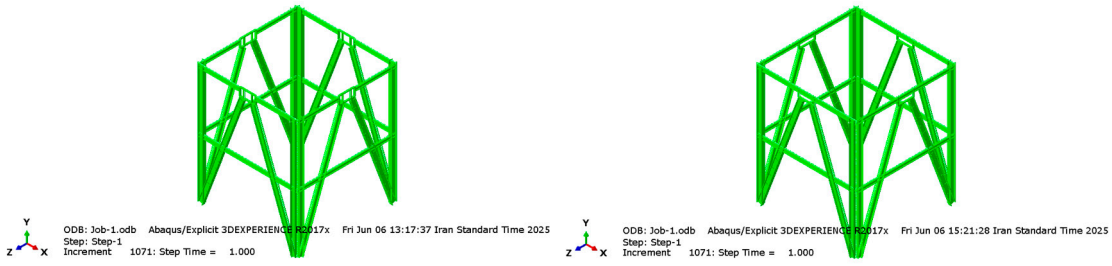

Figure 3. Two-story chevron mega-braced frame model: without shape memory alloy (SMA) elements (right) and with integrated SMA elements (left).

 doi:10.20944/preprints202604.1181.v1

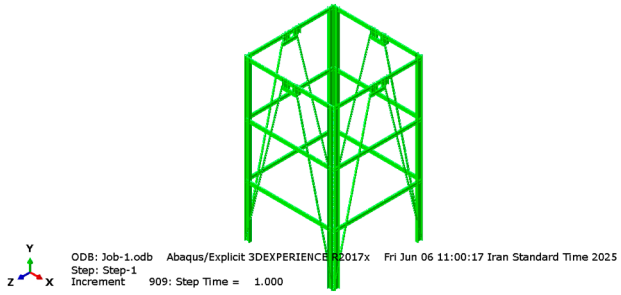

Figure 4. Three-story chevron mega-braced frame model with integrated shape memory alloy (SMA) elements.

The investigated models depicted in the figures above feature a bay width of 5 m. The cross sections adopted for the 2-story model consist of IPE240 profiles for beams and columns, supplemented with 200 × 8 cm stiffening plates of 2 cm thickness. The 3-story model employs IPE270 sections, while the 6-story models utilize IPB330 sections for beams and columns. For bracing members, channel sections C14, C16, and C18 are used from the roof level downward, respectively, as optimally designed sections. The repetition pattern of mega-bracing in the 6-story model follows the configurations illustrated in the subsequent figures.

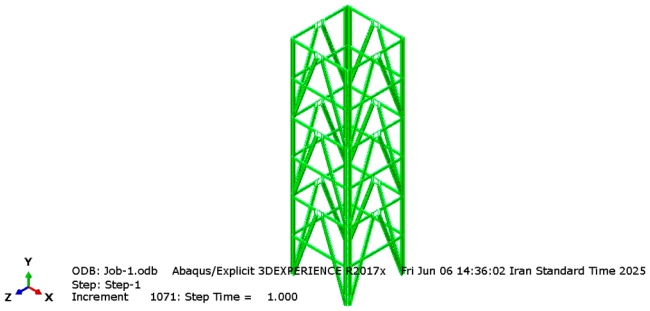

Figure 5. Six-story model with two-story repeated chevron mega-bracing integrated with shape memory alloy (SMA) elements.

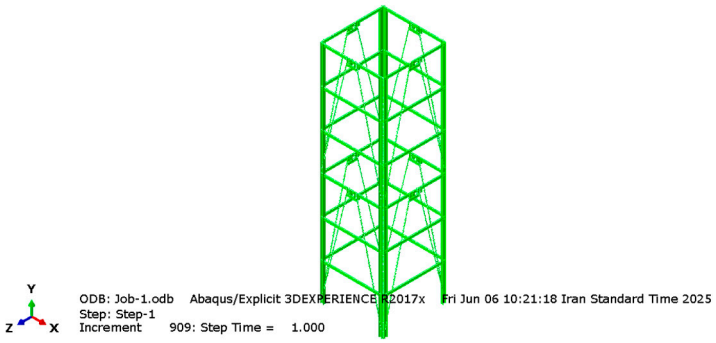

Figure 6. Six-story model with three-story repeated chevron mega-bracing integrated with shape memory alloy (SMA) elements.

Lateral forces are typically applied axially at beam-to-column connections. However, in reality, earthquake forces are not this simplistic; they exhibit quasi-static characteristics that subject the structure to severe high stresses, thereby rendering the estimation of the system's dynamic response highly significant [17]. In this study, boundary conditions were defined such that the base connections of the structure were modeled as fixed supports to ensure complete transfer of seismic forces into the structural system. Furthermore, to prevent rigid-body movement out-of-plane, the

 doi:10.20944/preprints202604.1181.v1

translational degrees of freedom of all model nodes were restrained in the direction perpendicular to the structural plane. Dynamic loading was applied based on a displacement-controlled history, as shown in Figure 8. This loading protocol simulated the Maximum Considered Earthquake (MCE) intensity level by incorporating three-stage loading–unloading cycles (positive–zero–negative) with a maximum displacement equivalent to 4.5% of the total structural height, in accordance with FEMA P695. This approach was selected due to its compatibility with cyclic behavior assessment and self-centering evaluation, as well as its capacity for precise control of interstory drift demands.

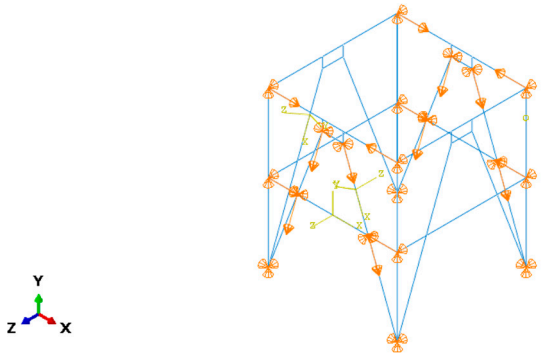

Figure 7. Loading and boundary conditions for the 2-story braced model without shape memory alloy (SMA) elements.

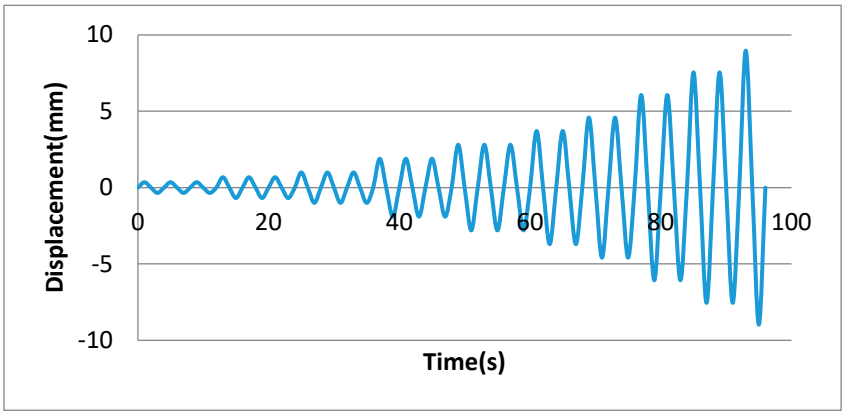

Figure 8. Displacement-controlled loading history.

For comparative evaluation of the investigated models, the behavior factor and residual displacements were employed as primary response indicators. According to FEMA 356, the behavior factor is derived as the product of the ductility factor and the overstrength factor.

The numerical model was validated against experimental results reported by Jia et al., who investigated the seismic performance of shape memory alloy elements integrated with metallic braces [9]. Specimen "b," illustrated in Figure 9, comprised a fixed anchorage plate and a brace subjected to tension connected to a moving plate.

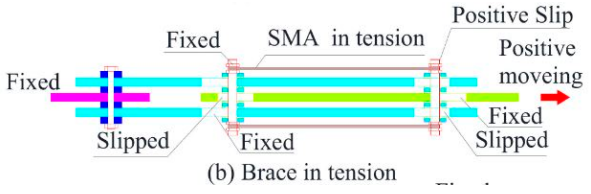

 doi:10.20944/preprints202604.1181.v1

Figure 9. Geometry of specimen "b" from Jia et al. [9].

The dimensions and size of the plate are shown in Figure 10.

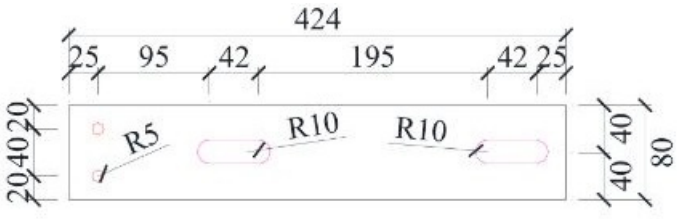

Figure 10. Dimensions and size of the plate [9].

The specimen parameters are presented in Table 4. The specimens were defined by four parameters: slip bolt torque, SMA wire cross-sectional area, SMA wire loading rate, and initial SMA wire strain. Across all specimens, the slip bolt torque and SMA area were consistently set to 10 N·m and 43.96 mm², respectively. For instance, specimen "SCB-12-25" denotes a self-centering brace subjected to a loading rate of 0.0012 s^{-1} and an initial strain amplitude of 0.25%. The influence of loading rate on the seismic performance of the SMA self-centering brace was investigated through specimens SCB-12-0, SCB-18-0, SCB-24-0, and SCB-36-0, while the effect of initial strain was examined using specimens SCB-12-0, SCB-12-25, SCB-12-50, and SCB-12-100.

Table 4. Characteristics of experimental specimens from the validation study [9].

No.	Specimen Name	Torque (N·m)	SMA Area (mm²)	Loading Rate (s^{-1})	Initial Strain (%)
1	SCB-12-0	10	43.96	0.0012	0.00
2	SCB-18-0	10	43.96	0.0018	0.00
3	SCB-24-0	10	43.96	0.0024	0.00
4	SCB-36-0	10	43.96	0.0036	0.00
5	SCB-12-25	10	43.96	0.0012	0.25
6	SCB-12-50	10	43.96	0.0012	0.50
7	SCB-12-100	10	43.96	0.0012	1.00

Table 5. Mechanical properties of steel plates [9].

No.	Thickness (mm)	Yield Strength (MPa)	Tensile Strength (MPa)	Young's Modulus (GPa)	Elongation (%)
1	8	365	545	206	23.1
2	15	372	556	209	25.2

Cyclic loading tests were conducted using an SDS100 fatigue testing machine at the Mechanical Engineering Testing Center of Nanchang University. The experimental setup comprised four main components: sensors, a control station, a control terminal, and signal connectors, as illustrated in Figure 11. The machine is capable of applying a maximum hydraulic load of 100 kN with an accuracy of 0.01 kN. The lower plate of the testing machine was connected to the fixed plate, while the upper plate was attached to sliding plate I of the SMA self-centering brace. Load and displacement responses of the test specimens were directly recorded by the sensors. All experiments were carried out at an ambient temperature of 27°C [9].

 doi:10.20944/preprints202604.1181.v1

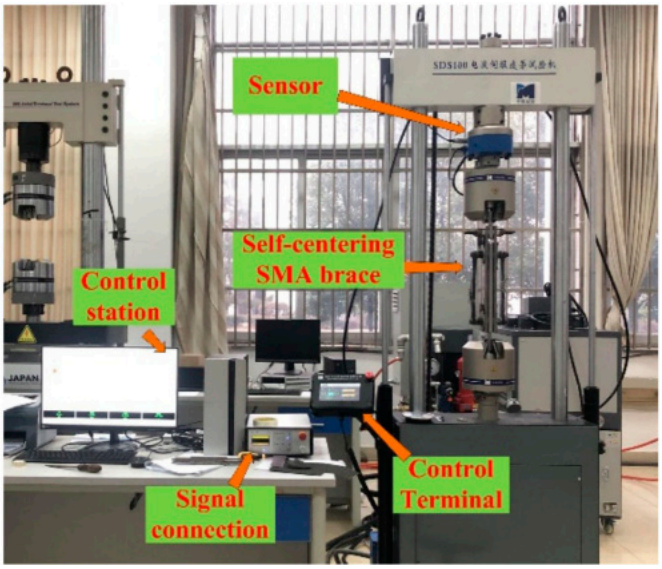

Figure 11. Testing apparatus of the validation study [9].

The validation model was developed in ABAQUS software. The SMA wire with a diameter of 1 mm was procured from Gao'an SMA Material Co., Ltd., as employed in the validation study, with the chemical composition reported in reference [9] confirming that the utilized SMA is a high-purity nickel–titanium (Ni–Ti) alloy. This alloy is commonly adopted in structural applications owing to its superelasticity and shape memory effect. The SMA material properties were implemented using the UMAT subroutine, consistent with the modeling approach adopted for the investigated structural frames. A comparison between the experimental results and the numerical ABAQUS simulation is presented in Figure 12.

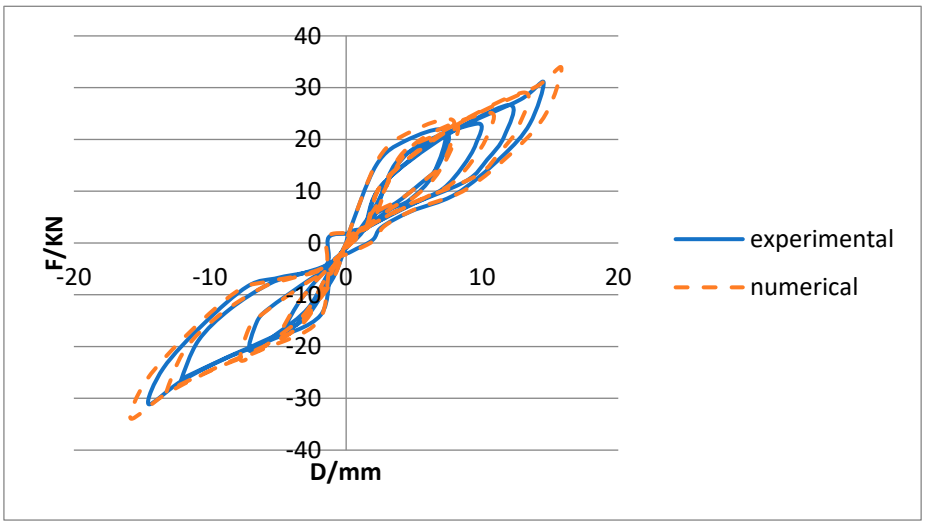

Figure 12. Comparison of validation model results with experimental data from Jia et al.

As shown in Figure 12, the two hysteretic loops exhibit close agreement in terms of shape, enclosed energy area, and quantitative response values, thereby confirming the validity and accuracy of the numerical model.

Following model validation and verification of the analysis platform, residual displacements and behavior factor were employed as primary performance indicators in this study. The behavior factor (*R*), a key metric for seismic performance evaluation, was calculated in accordance with FEMA 356 (2000). According to this methodology, the capacity curve obtained from nonlinear static (pushover) analysis was idealized into a bilinear form. The yield point (*Vy*, *Dy*) was determined by constructing a line passing through the origin and intersecting the capacity curve at a point

 doi:10.20944/preprints202604.1181.v1

corresponding to 60% of the maximum strength; the intersection of this line with the actual capacity curve was defined as the yield point. Subsequently, the ductility factor (μ) was computed as the ratio of ultimate displacement (*D*u) to yield displacement (*D*y), and the overstrength factor (Ω0) was calculated as the ratio of maximum strength (*V*max) to yield strength (*V*y). Finally, the behavior factor was obtained using the following expression:

$$R = \mu.\Omega_0 \quad (1)$$

4. Analysis Results

The analysis results for the models introduced in ABAQUS are presented in the following figures. The investigated models comprise four configurations across 2-, 3-, and 6-story frames equipped with mega-braces and shape memory alloy (SMA) elements, with their respective capacity curves illustrated below.

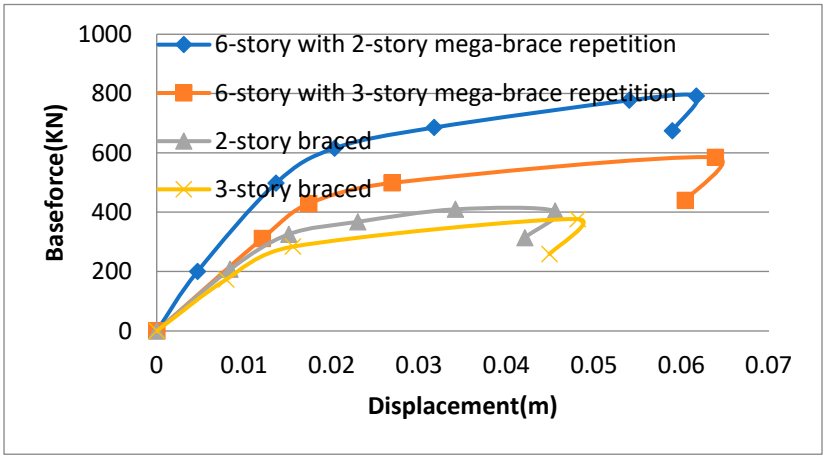

Figure 13. Comparison of capacity curves for the investigated models without SMA.

According to the capacity curve of the 6-story model with two-story mega-bracing (without SMA), it exhibits greater energy absorption compared to the 3-story braced model. Based on the calculated area under the force–displacement curve, the 2-story mega-braced model demonstrates approximately 31% higher energy absorption than the 3-story braced configuration. In the 6-story model, the two-story bracing repetition pattern shows superior performance compared to the three-story bracing repetition pattern.

 doi:10.20944/preprints202604.1181.v1

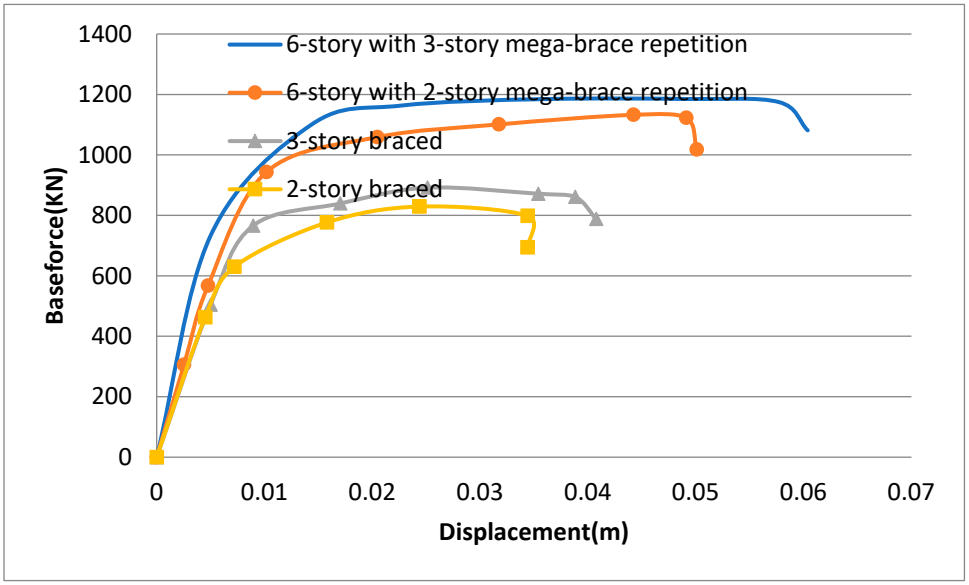

Figure 14. Comparison of force–displacement curves for the investigated models with SMA.

Based on the capacity curve, the 6-story model with two-story mega-bracing and SMA reaches collapse at a displacement of 4.9 cm, exhibiting a 41% reduction in energy absorption compared to the corresponding model without SMA. The 6-story model with three-story mega-bracing and SMA collapses at a displacement of 5.7 cm. The 3-story mega-braced model with SMA collapses at 3.8 cm displacement, demonstrating a 7% increase in earthquake energy absorption relative to the 2-story SMA-equipped model, which collapses at 3.4 cm displacement.

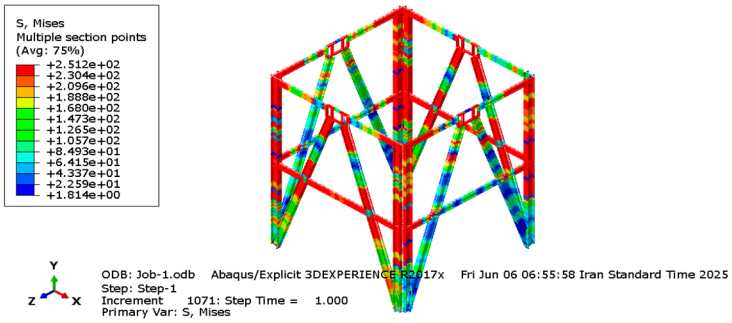

Figure 15. Stress contour of 2-story Megabrace Chevron brace model with SMA.

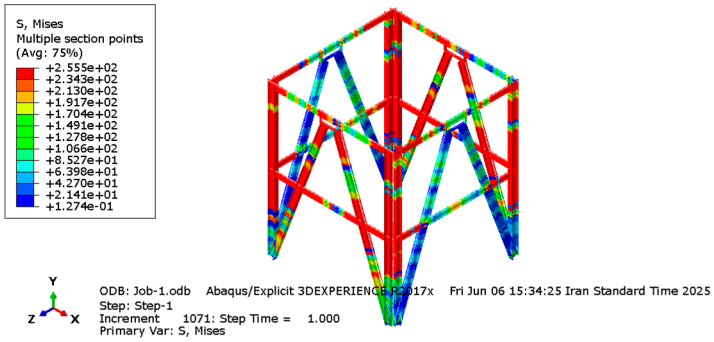

Figure 16. Stress contour of the 2-story Megabrace Chevron brace model without SMA.

According to the stress contours in the 8-shaped megabris braces in two stories braced in one opening, it shows that in the maximum stress, there is a 98% reduction in stress in the model with shape memory alloy, and in the minimum stress, it increases by 12% in the model without shape

 doi:10.20944/preprints202604.1181.v1

memory alloy. As it shows, SMA provides better stress distribution along the length of the member. This property causes a better distribution of stress along the brace member and prevents the concentration of stress in certain points (such as joints or nodes.(

On the other hand, the presence of SMA showed the reduction of maximum stresses due to energy absorption. SMA can absorb a lot of energy during deformation, which reduces stress fluctuations during seismic periods. Therefore, peak stresses in structural members such as columns and beams are reduced. The use of SMA in megabris braces reduces destructive and residual stresses and optimizes stress distribution. This, along with the increase in ductility and energy absorption, leads to an improvement in the overall seismic performance of the structure and an increase in the behavior coefficient.

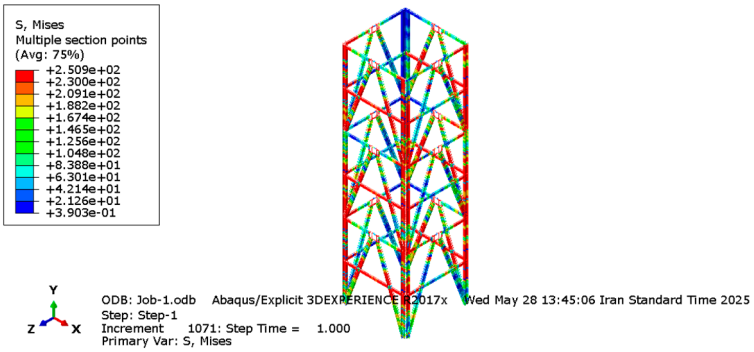

Figure 17. Stress contour of the 6-story model with two stories of Megabrace Chevron brace with SMA.

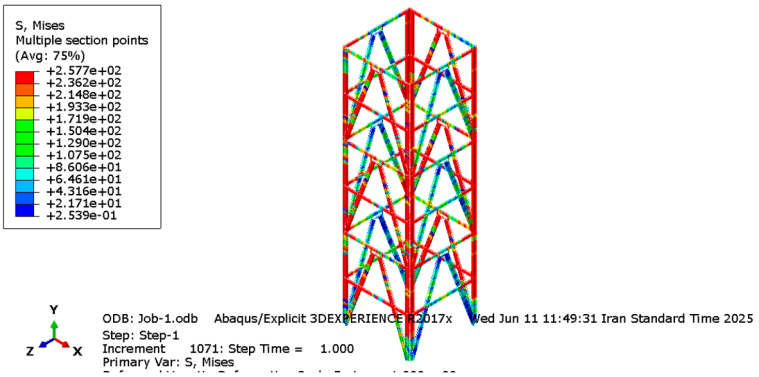

Figure 18. Stress contour of the 6-layer model with two layers of Megabrace Chevron brace without SMA.

In the contours of 6 floors with two floors, Chevron Megabrace braces are effective in the presence of SMA, and the highest stresses in the model with SMA show a 97% reduction in Mises stress compared to the model without SMA. Also, in the results of the models such as the 2-story model, in the presence of SMA, the minimum Mises stress increases by 64%. It showed the highest stresses on the vertical members due to the buckling load of the braces. The analysis of Mises stress contours in 6-story structures with 8-shaped megabrace braces showed that the use of shape memory alloys (SMA) has a direct effect on the distribution and amount of stress in structural members. In general, the model with SMA has experienced a 98% reduction in maximum Mises stress compared to the same model without SMA. These stress results are visible especially in the critical areas of the structure (such as the beam-to-column junction) and indicate smoother performance and better energy absorption in the presence of SMA.

On the other hand, in examining the results of the braced 2-story model, the use of SMA has been associated with a 21% increase in the minimum value of Mises stress. This phenomenon can be attributed to the quasi-elastic behavior of SMA; Because this alloy enters the nonlinear range in initial loads and absorbs initial stresses, while in some low stress areas, the increase in stress is noticeable

 doi:10.20944/preprints202604.1181.v1

due to redistribution of forces and increase in local hardness. It has also been observed that the highest stresses are mainly in the vertical members and due to the buckling load caused by the performance of the braces. This indicated that the out-of-plane or under-pressure bearing in the braces caused the transfer of concentrated stresses to the vertical members, which should be carefully considered in the design of the structure to avoid local failure.

Therefore, SMA, as a smart material, reduces concentrated stresses in critical areas and thus can reduce the possibility of local damage. The local increase of smaller stresses in some areas in the presence of SMA can be a sign of improved force distribution in the whole system. Structural designers should pay special attention to accurate analysis of buckling stresses and force transfer between members when using SMA.

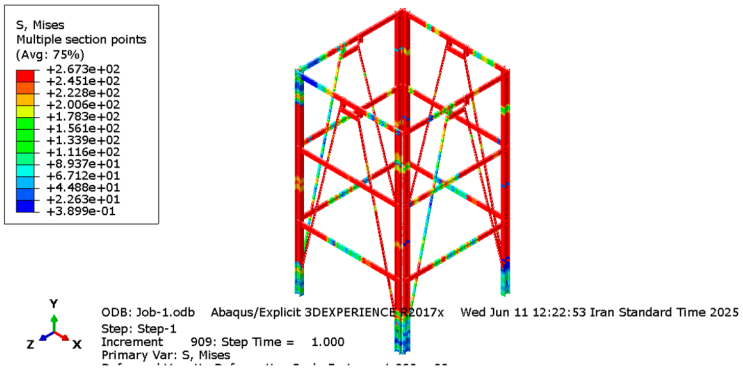

Figure 19. Stress contour of the 3-story model of Megabrace Chevron brace without SMA.

In the 3-story megabriss bracing model, it shows that the maximum Mises stresses occur in the columns and beams. The buckling load on the brace also caused the maximum stress on the compression member of the brace.

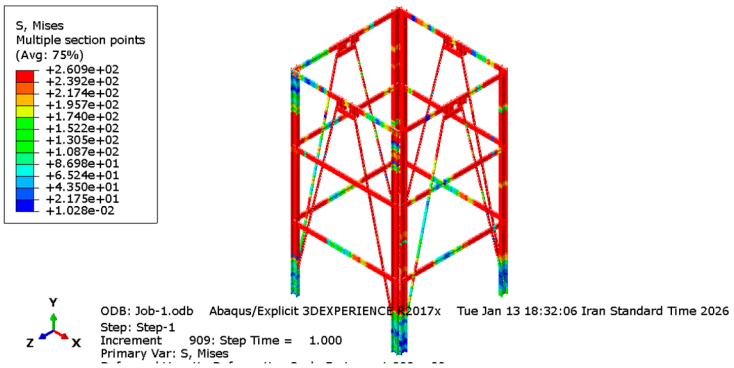

Figure 20. Stress contour of the 3-story model of Megabrace Chevron brace with SMA.

In the results of the Mises stress in the 3-story models, the highest stress was obtained with the presence of SMA, a 98% decrease compared to the model without SMA. The lowest Mises stress in the 3-story model braced with Chevron Megabrace was not significantly changed by the presence of SMA.

According to Figures 21 and 22, the highest amount of stress was reduced by 95% with the presence of SMA in the 6-story model with two stories braced by Chevron Megabrace. In the lowest value of the resulting stress in two models, an insignificant value was obtained.

 doi:10.20944/preprints202604.1181.v1

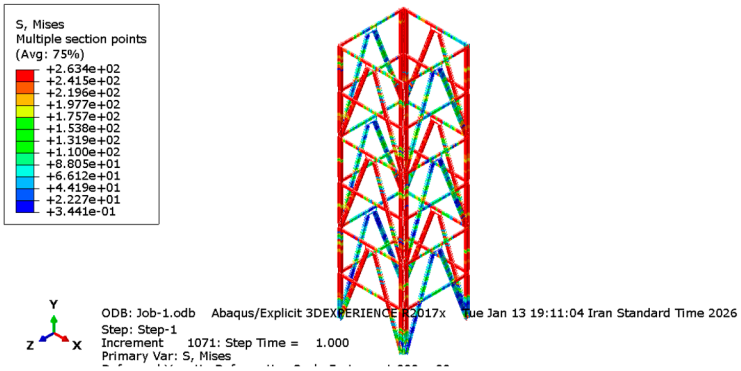

Figure 21. Stress contour of 6-layer model with 2 layers of Megabrace Chevron brace without SMA.

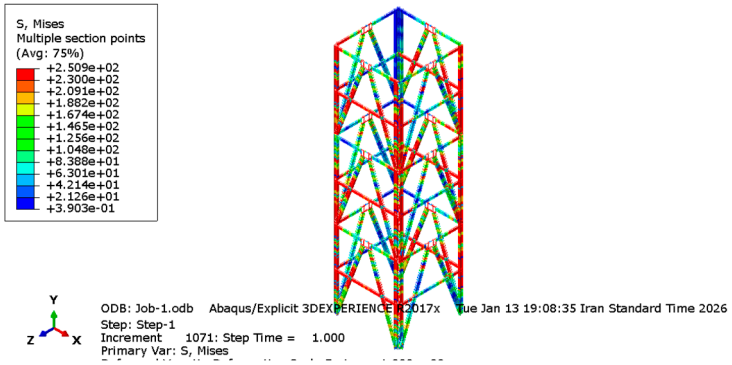

Figure 22. Stress contour of 6-story model with 2-story Megabrace Chevron brace with SMA.

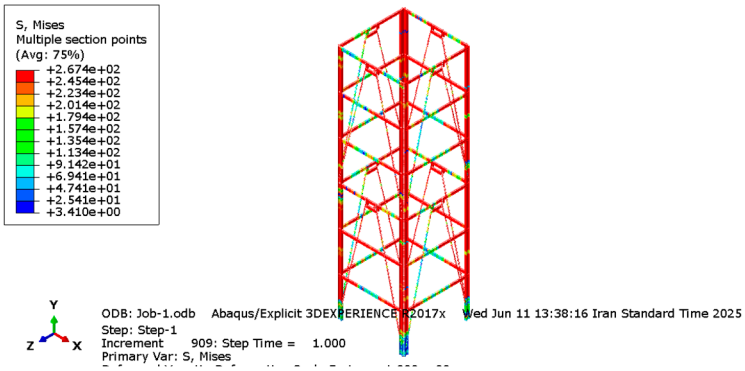

Figure 23. Stress contour of 6-layer model with 3 layers of Megabrace Chevron brace without SMA.

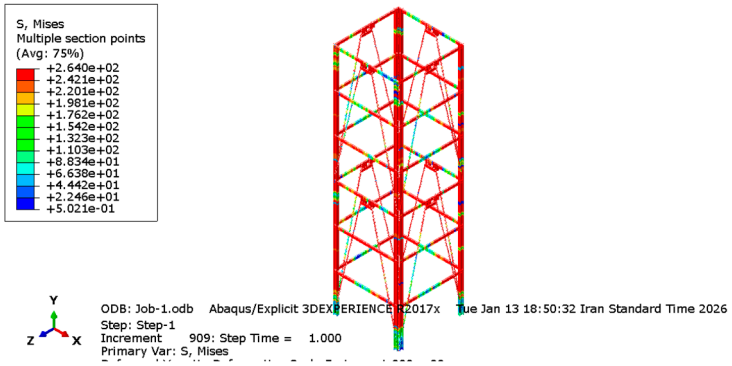

Figure 24. Stress contour of 6-story model with 3-story Chevron megabrace brace with SMA.

 doi:10.20944/preprints202604.1181.v1

According to the Meiss stress contours, the stress results show the same performance as the two-story models, and the reduction of the shear force of the beams and the transfer to braces, columns, and vertical members is more obvious. The lowest Mises stress in the model with SMA decreased by 14% compared to the model without SMA. This conclusion showed the opposite behavior in the three-story and two-story model. In other words, the minimum Mises stress was obtained by reducing the stress in the 6-story model with SMA compared to without considering it. The presence of memory alloy (SMA) in structures equipped with megabris braces not only reduces the overall stress and return of deformation, but also effectively prevents the concentration of stress in critical points such as connection nodes, ends of braces, plates and beam-to-column joints. This occurs due to the nonlinear elastic and superelastic behavior of SMA; Because this material deforms greatly under seismic loads, but without causing permanent yielding, it generates restoring forces and transfers these forces more uniformly throughout the system. In conventional structures, large deformations lead to stress concentration in weak areas or stiff nodes, which increases the probability of weld cracking, local buckling, or sudden failure. But in systems with SMA, due to the intelligent flexibility and the ability to withstand high strain, the stresses were distributed throughout the SMA element and scattered in other members instead of being concentrated in one point. This balanced distribution of stress prevents the formation of a "failure path" at one point and leads the behavior of the structure towards integrated and stable performance. Especially in megabris braces, where very high forces are concentrated in the central nodes, the presence of SMA as an energy absorber with the ability to return, reduced the pressure on these sensitive points and reduced premature fatigue and cracks caused by stress concentration. Therefore, SMA not only restores the structure better, but also significantly improves the safety and durability of the structure against seismic cyclic loads by preventing stress concentration.

Table 5. Comparison of the results of the examined models.

Parameter	Compared Models	Changes with SMA (%)	Technical Explanation
Energy Absorption	6-story + 2-story braced frame (without SMA) vs. 3-story braced frame (without SMA)	+31% (2-story model)	The 2-story model equipped with mega-braces (without SMA) exhibits higher energy absorption capacity compared to the 3-story braced configuration.
Energy Absorption	6-story + 2-story braced frame (with SMA) vs. identical model (without SMA)	+41%	Incorporation of SMA results in a significant enhancement in energy absorption, likely attributed to improved ductility and optimized superelastic behavior of the SMA elements.
Energy Absorption	3-story braced frame (with SMA) vs. 2-story braced frame (with SMA)	+7%	The 3-story SMA-equipped model demonstrates superior energy absorption relative to the 2-story counterpart, indicating enhanced SMA performance efficiency in mid-rise structural configurations.
Energy Absorption	6-story + 3-story braced frame (with SMA) vs.	-50%	SMA integration reduces the displacement capacity prior to collapse, suggesting a

 doi:10.20944/preprints202604.1181.v1

	identical model (without SMA)		trade-off between energy absorption and ultimate drift capacity.
Von Mises Stress (Max)	2-story braced frame (with SMA) vs. without SMA	-98%	Notable reduction in peak stress indicates improved stress redistribution and mitigation of stress concentration at critical connection zones.
Von Mises Stress (Min)	2-story braced frame (with SMA) vs. without SMA	+12%	Variation in minimum stress reflects the nonlinear elastic response of SMA and localized stiffness enhancement within the bracing system.
Von Mises Stress (Max)	3-story braced frame (with SMA) vs. without SMA	-97%	Substantial reduction in maximum stress demonstrates effective stress mitigation through SMA's flag-shaped hysteresis and recentering capability.
Von Mises Stress (Min)	3-story braced frame (with SMA) vs. without SMA	0%	Negligible variation in minimum stress values, indicating stable baseline stress conditions under cyclic loading.
Von Mises Stress (Max)	6-story + 2-story braced frame (with SMA) vs. without SMA	-95%	Moderate reduction in peak stress suggests smoother hysteretic response and enhanced energy dissipation efficiency with SMA integration.
Von Mises Stress (Min)	6-story + 2-story braced frame (with SMA) vs. without SMA	0%	Insignificant change in minimum stress, confirming consistent elastic baseline behavior in the hybrid system.
Von Mises Stress (Max)	3-story braced frame (with SMA) vs. without SMA	-98%	Reduction in peak stress coupled with improved force distribution uniformity across the structural system equipped with SMA braces.
Von Mises Stress (Min)	6-story + 3-story braced frame (with SMA) vs. without SMA	-14%	Decrease in minimum stress indicates more stable post-yield behavior and optimized stress distribution in taller structural configurations.
Energy Dissipation (Hysteresis)	Models with SMA vs. without SMA	≈ Identical	SMA demonstrates excellent seismic energy absorption capacity; however, no significant difference is

 doi:10.20944/preprints202604.1181.v1

observed in hysteretic energy dissipation, reflecting the superelastic flag-shaped response and inherent energy recovery characteristics of SMA materials.

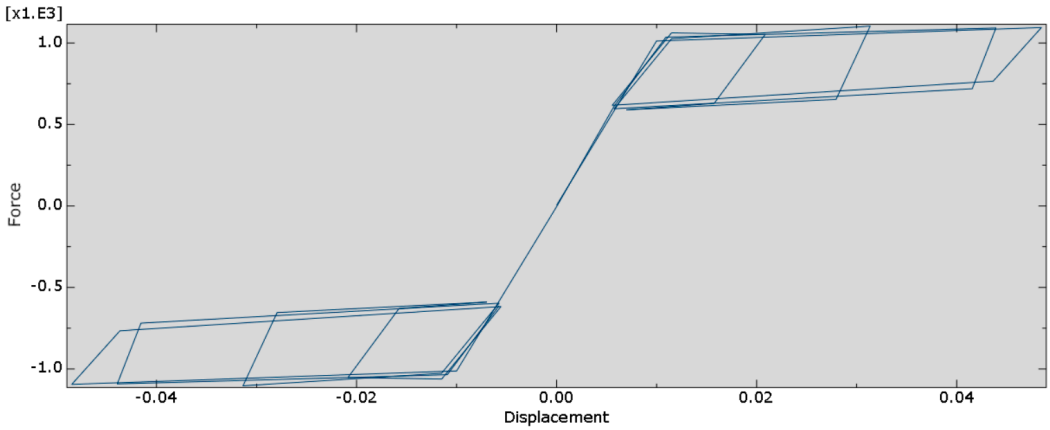

Figure 31. A view of the graphical output from ABAQUS model of 6 floors with two floors of megabrace bracing with shape memory alloy.

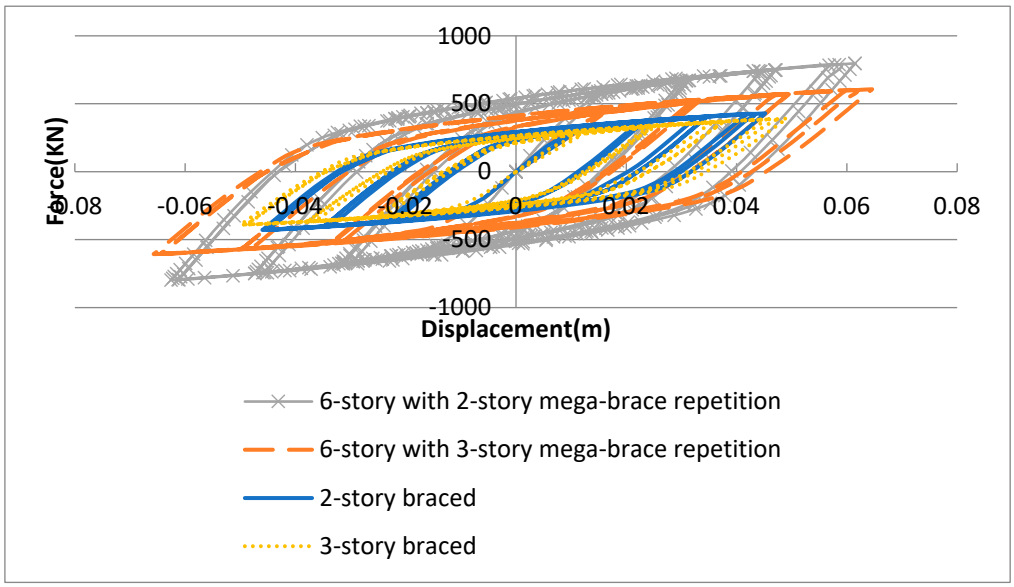

Figure 32. Hysteresis curves of different two- and three-story bracing models without SMA.

The observed 41% enhancement in energy dissipation for the two-story braced configuration suggests that strategic placement of SMA-enhanced mega-braces at lower stories may optimize hysteretic performance while maintaining favorable force distribution mechanisms in Chevron-braced steel frames.

 doi:10.20944/preprints202604.1181.v1

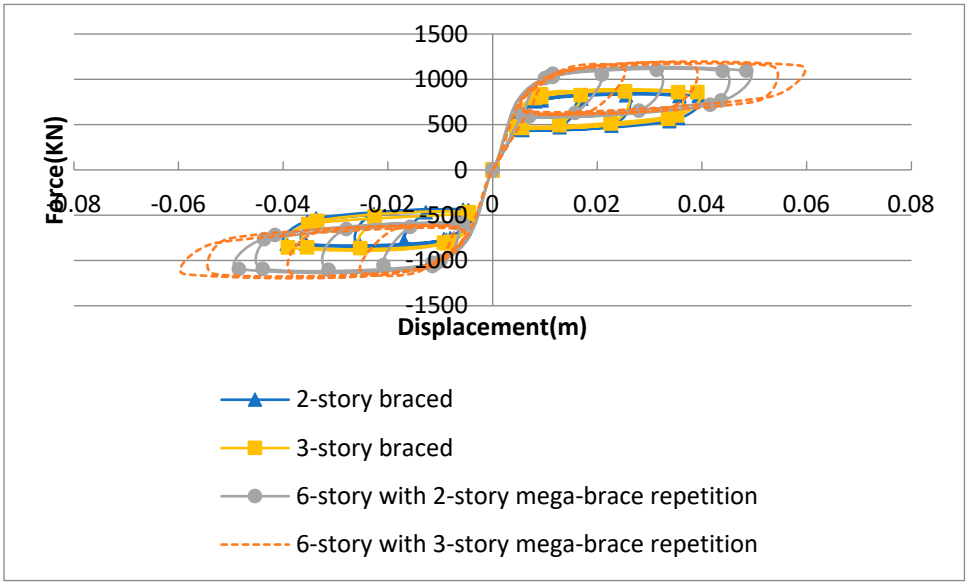

Figure 33. Hysteresis curves of different two- and three-story bracing models with SMA.

The 21% enhancement in hysteretic energy dissipation for the three-story braced configuration in SMA-equipped 6-story frames suggests that SMA utilization modifies the force redistribution mechanism and extends the effective yielding range across multiple stories. This performance gain rationalizes the reversal of design preference from two-story to three-story bracing highlighting the importance of considering SMA-induced superelasticity in the seismic optimization of mid-rise Chevron-braced steel frames.

Table 6. Changing the locations of the roof floor waste in the research models.

Structural Model	Configuration	Residual Roof Displacement (mm)	Residual Displacement Reduction vs. Non-SMA Model (%)
2-story frame	Without SMA	−4.68	—
2-story frame	With SMA	+0.005	≈ 99.9%
3-story frame	Without SMA	−4.64	—
3-story frame	With SMA	+0.005	≈ 99.9%
6-story frame (2-story braced)	Without SMA	−6.97	—
6-story frame (2-story braced)	With SMA	+0.006	≈ 99.9%
6-story frame (3-story braced)	Without SMA	−6.95	—
6-story frame (3-story braced)	With SMA	+0.007	≈ 99.9%

The observed dependency of residual displacements on the fundamental period aligns with established dynamics principles: longer-period (taller) structures experience larger displacement demands under far-field ground motions. The drastic mitigation of residual drifts in SMA-equipped models regardless of height underscores the self-centering efficiency of superelastic braces, which recover large inelastic deformations through reversible phase transformation (austenite ↔

 doi:10.20944/preprints202604.1181.v1

martensite). This performance advantage directly supports higher target performance levels (e.g., Immediate Occupancy or Operational) in FEMA 356-based assessments, potentially justifying elevated R-factors for SMA-braced systems pending experimental validation and code acceptance.

Table 7. The coefficient of behavior of the investigated models.

Structural Model	Configuration	Behavior Factor (R) per FEMA 356
6-story frame (2-story braced)	With SMA	5.91
6-story frame (2-story braced)	Without SMA	2.20
6-story frame (3-story braced)	With SMA	2.70
6-story frame (3-story braced)	Without SMA	2.80
3-story frame	With SMA	5.30
3-story frame	Without SMA	4.10
2-story frame	With SMA	2.30
2-story frame	Without SMA	2.20

In this research, the behavior coefficient (R) was extracted based on the FEMA 356 standard method and through bilinear idealization of the capacity curve. Based on this, first a line was drawn from the origin of the curve to pass through a point where the basic shear force is equal to 60% of the maximum resistance (0.6Vmax). The intersection of this line with the real curve was considered as the yield point (Dy,Vy). The ultimate displacement (Du) was also defined as the point at which the base shear force was significantly reduced and the system entered the softening stage.

In the case of systems equipped with shape memory alloy (SMA), yield displacement (Dy) showed smaller values than similar structures without SMA. This phenomenon is caused by the inherent nonlinear behavior of SMA; So that even in small strains, the phase transformation of austenite to martensite occurs and the system leaves the linear behavior. As a result, the computational ductility ($\mu=Du/Dy$) increases, which leads to an increase in the behavior coefficient ($R=\Omega 0\times\mu$). This increase, as observed in the 6-story model with two bracing floors (163% increase from 2.25 to 5.91), indicates the improvement of energy absorption and ductility of the SMA megabriss composite system.

Table 8. Comparison and interpretation of the behavior coefficient results of the investigated models.

Structural Model	R-Factor (with SMA)	R-Factor (without SMA)	Increase in R with SMA (%)	Technical Interpretation
6-story frame (2-story braced)	5.91	2.25	+163%	SMA integration substantially enhanced seismic performance, attributed to optimal bracing distribution and effective mobilization of superelastic energy dissipation mechanisms.
6-story frame (3-story braced)	2.71	2.78	−2.5%	SMA exhibited negligible influence on the behavior factor, likely due to excessive global stiffness or suboptimal vertical distribution of bracing elements limiting SMA strain demand.

 doi:10.20944/preprints202604.1181.v1

3-story frame	5.31	4.10	+29.5%	SMA improved seismic response modification capability; however, the enhancement was less pronounced compared to the 6-story/2-story braced configuration, suggesting height-dependent efficiency of SMA braces.
2-story frame	2.33	2.21	+5.4%	SMA demonstrated marginal improvement in R-factor, indicating reduced effectiveness in low-rise structures where fundamental periods are short and displacement demands are limited.

As seen in Table (5), the use of SMA has led to a decrease in ductility (μ) and behavior coefficient (R). However, these results indicate an improvement in structural performance, as the system uses superelastic behavior to absorb energy instead of entering the plastic region, reducing residual displacement to almost zero. This feature leads the structure to self-centering systems, which are much more favorable in terms of safety and economy (reduced need for repair(

5. Conclusions

This research demonstrated that integrating shape memory alloy (SMA) elements into chevron-type mega-bracing systems yields highly effective self-centering behavior; residual displacements in all 2-, 3-, and 6-story models were reduced by more than 99.9% on average. This characteristic enables the preservation of post-earthquake serviceability.

The incorporation of SMA not only significantly reduced plastic strains (up to 55% in the 6-story model with three-story mega-brace repetition) but also moderated stress concentrations and promoted a more uniform force distribution throughout the structure. This effect diminishes the potential for plastic hinge formation and enhances overall structural ductility.

Although SMA integration led to a reduction in the behavior factor (R) in certain models, this outcome does not reflect diminished energy dissipation capacity. Rather, it signifies a shift from plastic hysteresis toward superelastic energy absorption. This mechanism prevents the structure from entering severe plastic ranges and thereby mitigates permanent damage.

The influence of SMA on structural response is strongly dependent on bracing geometry—specifically, the number of stories spanned by each mega-brace unit. For instance, in taller structures (6 stories), the three-story mega-brace configuration exhibited superior performance in the presence of SMA, particularly in terms of plastic strain reduction and cyclic stability. Nevertheless, these findings are valid only for the present modeling conditions (single bay, uniform story height, chevron geometry), and broader generalization requires further investigation.

Limitations of this study include the omission of soil–structure interaction effects, lack of long-term fatigue assessment of SMA under repeated cyclic loading, and the use of simplified lateral loading protocols rather than actual earthquake records. Future research should evaluate these systems under near-fault ground motions and within more comprehensive three-dimensional modeling frameworks.

Overall, the proposed system—chevron mega-bracing integrated with SMA elements represents a promising solution for structures where damage mitigation, reduced repair costs, and post-

 doi:10.20944/preprints202604.1181.v1

earthquake functionality are prioritized. This innovation constitutes a significant step toward the development of highly reliable self-centering structures.

The principal innovation of this research lies in the concurrent integration of chevron mega-bracing systems with SMA elements and the comprehensive evaluation of this hybrid system's seismic performance specifically regarding residual drift reduction, plastic strain control, and influence on the behavior factor (R) across steel structures of varying heights (2, 3, and 6 stories). Unlike previous studies that examined SMA applications in conventional braces or localized connections from a component-level perspective, this work employs realistic three-dimensional modeling in ABAQUS with explicit dynamic analysis to assess the self-centering behavior systematically at the full structural scale. The findings demonstrate that such integration can virtually eliminate permanent deformations while maintaining cyclic stability and reducing stress concentrations, thereby paving the way for highly reliable structures capable of post-earthquake functionality.

References

1. Seyed Kazemi, A., Esmaeili, M., Iftikhar Ardebili, S., Hossein Ali Beigi, M., (2016), "The Effect of Smart Shape Memory Alloy Damper on Energy Dissipation and Vibration Amplitude Reduction of Multi-Story Steel Frames", Quarterly Journal of Structural Analysis - Earthquake, Volume 13, Issue 2. [in Persian].
2. Khati, Reza and Seyed Ghasem Jalali, (2019), Investigation of the fragility curve of three- and five-story steel frames equipped with off-axis bracing with a beam connection made of shape memory alloy materials and ordinary steel materials, Third International Conference on Applied Research in Structural Engineering and Construction Management, Tehran, Sharif University of Technology [in Persian].
3. Hu, J.W.(2013), Numerical simulation for the behavior of superelastic shape memory alloys, Journal of Mechanical Science and Technology, Vol. 27, No. 2, pp. 381-386
4. Khodabandeh Lou, Ashkan. (2024). Investigation of seismic behavior of steel convergent frame reinforced with arch-shaped braces in different installation positions in a two-story structure. Structural Engineering and Construction, 11(9), 213-237. doi: 10.22065/jsce.2024.425263.3274[in Persian].
5. Mardi. Ramin, Ghasemieh. Mehdi, (2023). Investigation and comparison of seismic behavior of modern metallic braces using incremental dynamic analysis method. Modares Civil Engineering, 23(2), 177-192.[in Persian].
6. Bagheri, Mansour; Amin Vedad and Seyed Hossein Ghodsi, (2020), Seismic performance evaluation of a double steel frame with divergent bracing equipped with shape memory alloy, 7th National Conference on Applied Research in Civil Engineering, Architecture and Urban Management and 6th Specialized Exhibition of Housing and Building Mass Producers of Tehran Province, Tehran - International Conference Center of Radio and Television, Khajeh Nasiruddin Toosi University of Technology.[in Persian].
7. Danesh, Masoud and Sanaz Jafari, (2020), Effect of joints equipped with shape memory alloy on superelastic vibration performance, National Conference on Building, Environment and Energy Consumption Management, Ahvaz, Shahid Chamran University of Ahvaz - Khuzestan Province Building Engineering System Organization - Khuzestan Industry, Mines and Trade Organization.[in Persian].
8. Zhou.Y, Shao.H, Cao.Y, Lui.E.M, (2021), Application of buckling-restrained braces to earthquake-resistant design of buildings: A review, Engineering Structures, Volume 246, 1 November 2021, 112991
9. Jia, Y., Zhang, B., Zeng, S., Tang, F., Hu, S., & Chen, W. (2022). Effect of loading rate and initial strain on seismic performance of an innovative self-centering SMA brace. Materials, 15(3), 1234.
10. Jena, S., Sahoo, D. R., & Yadav, D, (2025), Performance of Hybrid Fe-Sma Buckling-Restrained Braced Frames Under Far-Field and Near-Fault Earthquakes. Available at SSRN 5202132.
11. Houshmand, Mohammad, Rafizi, Behzad and Khalil Alafi, Jafar. (2013). Investigation of seismic behavior of steel structures using composite braces made of steel and shape memory alloys. Journal of Civil and Environmental Engineering, University of Tabriz, 43.3(72), 11-22.[in Persian].
12. Mahmoudi, M.,(2014), Seismic behavior of X-braced frames with shape memory alloys, Journal of Advances in Civil and Environmental Engineering, Vol. 2, No. 1, 2014, pp. 1 -19.

 doi:10.20944/preprints202604.1181.v1

13. Dieng, L., Helbert, G., Chirani, S.A., Pilvin Lecompte, T.,(2015), Use of shape memory alloys damper device to mitigate vibration amplitudes of bridge cables, Engineering Structures, Vol. 56, pp. 1547 -1556.
14. Lobo, P.S., Almeida, J. Guerreiro, L.,(2015), Semi-active damping device based on super-elastic shape memory alloys, Structures, Vol. 3, pp. 1-12.
15. Gur, S., Mishra, S.K., Roy, K.,(2015), Stochastic seismic response of building with super-elastic damper, Mechanical Systems and Signal Processing, , Article in Press.
16. Xinzheng Lu , Xiao Lu, Hong Guan, Wankai Zhang, Lieping Ye, (2013), Earthquake-induced collapse simulation of a super-tall mega-braced frame-core tube building, Journal of Constructional Steel Research 82 59–71.
17. Yang, C. S. W., DesRoches, R., & Leon, R. T. (2010). Design and analysis of braced frames with shape memory alloy and energy-absorbing hybrid devices. Engineering Structures, 32(2), 498-507.
18. Hoveidae, N. (2023). Response modification factor of SMA-based self-centering buckling-restrained braced frames. DOI:10.21203/rs.3.rs-3217308/v1